viscosities of mixed solutions may cause their segregation due to inhomogeneity of the shear rate in the gap; visual observations made during these experiments showed that this effect was hardly detectable. Instead, formation of small vertical vortexes (low viscosity ratio) and spots of different size (high viscosity ratio) was detected; these structures were similar to that observed by Murakami et al.[24] in a cone-plate mixer.

8.2.4. Effect of a Local Disturbance of a Unidirectional Couette Flow on the Product Distribution.

The shear flow produced in the annular gap between the cylinders tends to orient intermaterial surfaces along direction of shear. When it happens, both the rate of growth of the surface area and the rate of thinning of reactant layers drop to zero. To prevent this happening one should try to reorient the solution layers in the direction of the fastest stretching in the shear flow; this direction is deflected 45 degrees from the direction of shear - see discussion in chapter 3.1.

Two attempts were undertaken to modify the experimental system in such a way as to achieve a local reorientation of the shear flow in the annular gap.

In the first case (fourth series of experiments) 5.5 mm wide and 2 mm thick plate, extending between the bottom and the top cover of the reactor, was inserted in the middle of the annular gap. The baffle was made of stainless steel. The initial distribution of the substrates solutions and position of the plate are shown in figure 8.8. After filling the gap with solutions, rotation of the inner cylinder was initiated and kept constant for one hour. The experiments were conducted at 22°C. Tables 8.IVabc present compositions, amounts, viscosities and densities of solutions, together with rotational speeds and the final selectivities.

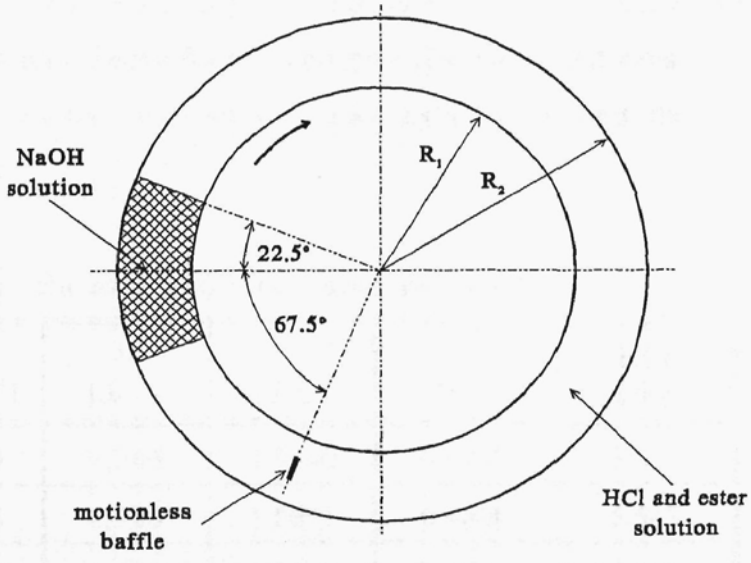

Figure 8.8. Initial distribution of the substrates solutions and position of the baffle in the gap.

In the second case (fifth series of experiments) a small, six-blades turbine, made of brass, was

mounted in the middle of the annular gap. The diameter of the turbine was equal to 10 mm and the width of its blades was equal to 1 mm. The clearance between the lower edge of blades and the reactor bottom was equal to 1 mm, whereas the upper edge of blades was 1 mm above the top cover of the inner cylinder. The vertical alignment and free rotation of the turbine was assured by two teflon bearings fixed in the top cover and the bottom of the reactor. The turbine was rotated by a separate DC motor, with a constant speed and in the same direction as the inner cylinder. The initial distribution of the substrates solutions and position of the turbine in the gap are shown in figure 8.9. After filling the gap with the substrates solutions rotation of the turbine and rotation of the inner cylinder were initiated simultaneously and kept constant for one hour. The experiments were conducted at 18°C. Tables 8.Vabc present compositions, amounts, viscosities and densities of solutions, rotational speeds of the turbine $\mathbf{n_T}$ and the inner cylinder **n**, and the final selectivities.

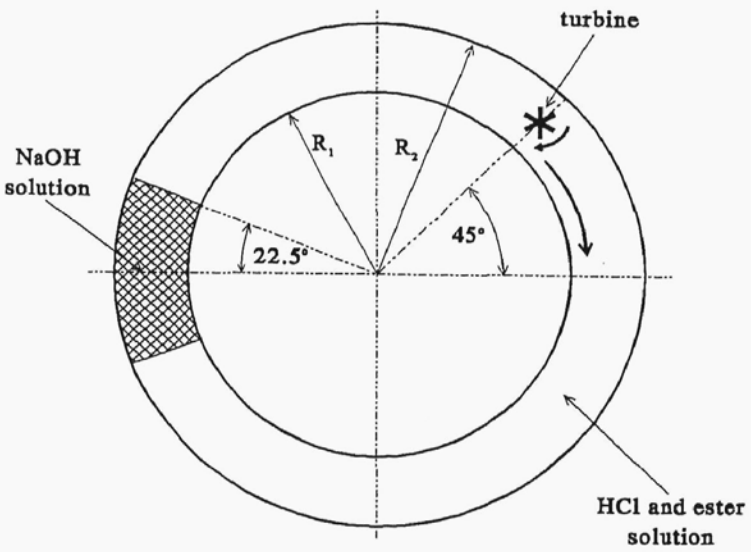

Figure 8.9. Initial distribution of the substrates solutions and position of the turbine in the gap.

Table 8.IVa. Fourth series of tests - the acid and ester solutions; w_P=42%.

Exp.no.	HCl [mol/dm^3]	Ester [mol/dm^3]	V [dm^3]	ρ [g/cm^3]	μ [Pa·s]	KCl [g/kg]
1	0.01389	0.01399	1.746	1.0690	0.4287	5.543
2	0.013976	0.01405	1.770	1.0691	0.4690	5.543
3	0.013976	0.01405	1.764	1.0691	0.4690	5.543
4	0.01393	0.01351	1.753	1.0690	0.4308	5.543

Table 8.IVb. Fourth series of tests - the base solutions; w_P=42%.

Exp.no.	NaOH [mol/dm^3]	V [dm^3]	ρ [g/cm^3]	μ [Pa·s]
1	0.09866	0.2550	1.0691	0.4565
2	0.09823	0.2514	1.0689	0.4542
3	0.09823	0.2430	1.0689	0.4542
4	0.09869	0.2616	1.0691	0.4503

Table 8.IVc. Fourth series of tests - final solutions after experiment.

Exp.no.	n [rev/min]	Ester [mol/dm^3]	X [%]	V [dm^3]	ρ [g/cm^3]	μ [Pa·s]
1	5	0.008658	28.19	2.001	1.0690	0.4363
2	10	0.008929	27.61	2.161	1.0690	0.4352
3	20	0.009135	27.02	2.007	1.0690	0.4337
4	40	0.08640	24.31	2.014	1.0688	0.4230

Table 8.Va. Fifth series of tests - the acid and ester solutions; w_P=42%.

Exp.no.	HCl [mol/dm^3]	Ester [mol/dm^3]	V [dm^3]	ρ [g/cm^3]	μ [Pa·s]	KCl [g/kg]
1	0.01436	0.01348	1.711	1.0717	0.5029	5.543
2	0.01436	0.01348	1.715	1.0717	0.5029	5.543
3	0.01457	0.01399	1.709	1.0717	0.5063	5.543

Table 8.Vb. Fifth series of tests - the base solutions; w_P=42%.

Exp.no.	NaOH [mol/dm^3]	V [dm^3]	ρ [g/cm^3]	μ [Pa·s]
1	0.09861	0.2423	1.0716	0.5420
2	0.09861	0.2408	1.0716	0.5420
3	0.09836	0.2429	1.0715	0.5235

Table 8.Vc. Fifth series of tests - final solutions after experiment.

Exp. no.	n [rev/min]	n_T [rev/min]	Ester [mol/dm^3]	X [%]	V [dm^3]	ρ [g/cm^3]	μ [Pa·s]
1	5	40	0.008439	27.55	1.954	1.0715	0.5018
2	10	40	0.008663	26.02	1.956	1.0716	0.5103
3	5	100	0.008976	26.70	1.952	1.0715	0.5080

To compare results of the forth series of experiments performed at 22°C with results of the first and the fifth series of experiments conducted at 18°C, a modified Damköhler number was introduced:

$$\overline{Da_S} = k_2 \cdot \bar{c}_{A0} \cdot t_{S1/2} \,, \tag{8.11}$$

where $\mathbf{k_2}$ is ester hydrolysis rate constant, $\bar{c}_{A0}$ stands for average initial concentration of sodium hydroxide in the reactor and $t_{S1/2}$ designates time required to reduce twice the concentration of NaOH, at the center of the deformed layer, due to molecular diffusion. In comparison to the standard definitions of Damköhler number, e.g. $\overline{Da} = k_2 \cdot \overline{c_{A0}}/n$ or $\overline{Da} = k_2 \cdot \overline{c_{A0}} \cdot s_0^2/D_A$, the present definition reflects influences of both diffusion and deformation. In a local coordinate system attached to a thinning lamina of the base solution, the differential material balance of NaOH with the boundary and initial conditions reads:

$$\frac{\partial c_A}{\partial t} + \frac{x}{s} \cdot \frac{ds}{dt} \cdot \frac{\partial c_A}{\partial x} = D_A \cdot \frac{\partial^2 c_A}{\partial x^2} \,, \tag{8.12a}$$

$$\left.\frac{\partial c_A}{\partial x}\right|_{x=0} = \left.\frac{\partial c_A}{\partial x}\right|_{x=s} = 0 \,, \tag{8.12b}$$

$$c_A(x,0) = \begin{cases} c_{A0} & 0 \le x < \delta_0/2 \\ 0 & \delta_0/2 \le x \le s_0 \end{cases} \,. \tag{8.12c}$$

In equations (8.12) **s** denotes the distance between the symmetry surfaces of neighboring laminas (the base lamina and acid-ester lamina). To simplify computations one can use the dimensionless variables:

$$\xi = \frac{x}{s} \,, \quad \textbf{(5.101a)} \qquad \tau = D_A \cdot \int_0^t \frac{dt'}{s(t')^2} \,, \quad \textbf{(5.101b)} \qquad C_i = \frac{c_i}{c_{A0}} \,. \quad \textbf{(5.101c)}$$

Substitution of variables (5.101) into equations (8.12) results in:

$$\frac{\partial C_A}{\partial \tau} = \frac{\partial^2 C_A}{\partial \xi^2}\,, \tag{5.79a}$$

$$\left.\frac{\partial C_A}{\partial \xi}\right|_{\xi=0} = \left.\frac{\partial C_A}{\partial \xi}\right|_{\xi=1} = 0\,, \tag{8.13a}$$

$$C_A(\xi,0) = \begin{cases} 1 & 0 \le \xi < \dfrac{\delta_0}{2s_0} \\ 0 & \dfrac{\delta_0}{2s_0} \le \xi \le 1 \end{cases}. \tag{8.13b}$$

Following Carslaw and Jaeger [65,p.101], the analytical solution of equations (5.79a) and (8.13) reads:

$$C_A(\xi,\tau) = \frac{\delta_0}{2\cdot s_0} + \frac{2}{\pi}\cdot\sum_{m=1}^{\infty}\frac{1}{m}\cdot\cos(m\cdot\pi\cdot\xi)\cdot\sin\left(\frac{m\cdot\pi\cdot\delta_0}{2\cdot s_0}\right)\cdot\exp\left(-m^2\cdot\pi^2\cdot\tau\right)\,. \tag{8.14}$$

Finally, in the case when $\delta_0/(2\cdot s_0)=1/8$, the "warped time" $\tau_{1/2}$ required to half the concentration of NaOH, at the symmetry surface of the base lamina, equals to 0.0172. In the experimental system the shear rate and consequently the value of **s** depends on a radial position, in the same way as δ given by equation (8.7). Thus, the real time $t_{S1/2}$ recalculated from expression (5.101b) will also be **r** dependent. In order to find the average value of $t_{S1/2}$ one should use in computations the average value of shear rate in the gap:

$$\bar{G} = \frac{1}{\pi\cdot\left(R_2^2 - R_1^2\right)}\cdot\int_{R_1}^{R_2} G(r)\cdot 2\cdot\pi\cdot r\,dr = 8\cdot\pi\cdot n\cdot\left(\frac{R_1\cdot R_2}{R_2^2 - R_1^2}\right)^2\cdot\ln\left(\frac{R_2}{R_1}\right)\,. \tag{8.15}$$

In this case, the average distance between the symmetry planes of neighboring layers reads:

$$\bar{s}(t) = \bar{s}_0 \Big/ \sqrt{1+\left(\bar{G}\cdot t\right)^2} \tag{8.16}$$

and the modified relation between the "warped time" and the real time is:

$$\tau = D_A\cdot\int_0^t \frac{dt'}{\bar{s}^2(t')}\,. \tag{8.17}$$

Considering the fact that the amount of polymer in the substrates solutions was slightly higher than 40%, the values of $\mathbf{k_2}$ used in computations of $\overline{\mathbf{Da_S}}$ were calculated as for water solution from equation (6.3); at 18 °C $\mathbf{k_2}$ equals to 23.7 $dm^3/(mol\cdot s)$ and at 22°C $\mathbf{k_2}$ equals to 28.8 $dm^3/(mol\cdot s)$. Diffusivity of sodium hydroxide was calculated from experimental correlation (6.14). For the experiments carried at 18°C (μ=0.51 Pa·s) one receives $\mathbf{D_A}=4.51\cdot10^{-10}$ m^2/s, whereas for the experiments conducted out at 22°C (μ=0.43 Pa·s) one

receives $\mathbf{D_A}$=5.02·10^{-10} m^2/s. The value of $\bar{s}$ at the beginning of the process was estimated from the following expression:

$$\bar{s}_0 = \frac{1}{2}\cdot\frac{1}{\pi\cdot\left(R_2^2 - R_1^2\right)}\cdot\int_{R_1}^{R_2}(2\cdot\pi\cdot r)^2\,dr = \frac{2\cdot\pi}{3}\cdot\frac{R_1^2 + R_1\cdot R_2 + R_2^2}{R_1 + R_2}\,. \qquad (8.18)$$

Figure 8.10 presents the final selectivities obtained in the first, fourth and fifth series of experiments plotted versus $\overline{\mathbf{Da}_S}$. Analysis of this figure shows considerable gain in mixing efficiency, due to the presence of the baffle in the annular gap, only for the lowest revolution speed (highest $\overline{\mathbf{Da}_S}$). A better improvement of mixing can be noticed in the case when the rotating turbine was used.

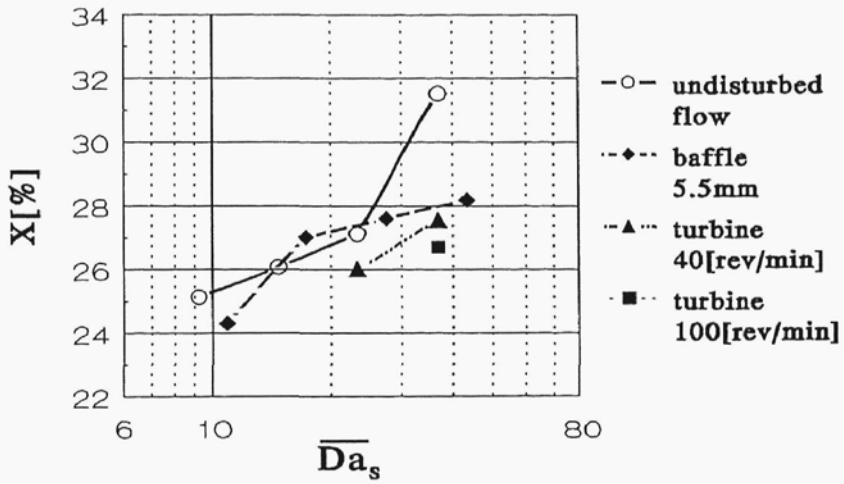

Figure 8.10. Effect of a flow disturbance on the product distribution in the batch reactor; first, fourth and fifth series.

8.2.5. Effect of a Local Disturbance of a Periodic Couette Flow on the Product Distribution.

A better improvement of mixing was achieved by means of motionless baffles for a periodic Couette flow. In this case the inner cylinder, instead of rotating in one direction, was oscillating with a constant frequency and amplitude. Experiments were conducted in three different ways:

1) without a baffle inserted in the annular gap between the cylinders,

2) with 5.5 mm wide and 2 mm thick baffle inserted in the middle of the gap,

3) with 18 mm wide and 2 mm thick baffle inserted in the middle of the gap.

The baffles were separated 67.5 degrees from the center of a zone initially occupied by the base solution, exactly as it is shown in figure 8.8. The lower edge of a baffle was fixed the reactor bottom, whereas the upper edge was fixed to the top cover of the reactor. The baffles were made of stainless steel. The initial position of the slider crank mechanism (figure 8.3)